ELSEVIER

Surface Science 391 (1997) L1217–L1223

surface science

Surface Science Letters

Image potential states on lithium, copper and silver surfaces

E.V. Chulkov [a,b,*], V.M. Silkin [a,b], P.M. Echenique [a]

[a] *Departimento de Fisica de Materiales, Facultad de Quimica, Universidad del Pais Vasco/Euskal Herriko Unibertsitatea, Apdo. 1072, 20080 San Sebastian, Spain*

[b] *Institute of Strength Physics and Materials Science, Russian Academy of Sciences, pr. Academicheskii 2/1, 634021 Tomsk, Russia*

Received 7 February 1997; received in revised form 11 August 1997; accepted for publication 11 August 1997

Abstract

The electronic structure of the Li(110) surface is calculated within the self-consistent pseudopotential method. The calculation does not give any occupied surface state. At the same time, unoccupied resonance surface states have been found at the $\bar{\Gamma}$ point and along the $\overline{\mathrm{PH}}$ symmetry directon. Image potential states with energies of $E_1 = -0.73$ eV and $E_2 = -0.22$ eV are predicted at the Γ point. For the description of the image potential states, we propose a one-dimensional model potential. The parameters of this potential are determined with the use of experimental (or first-principles calculation) values of the width and position of the energy gap at the $\bar{\Gamma}$ point and the energies E_0 and E_1 of the surface state and first image potential state, respectively. Using this model potential, we study the binding energies, wave functions and lifetime of image potential states on the Li(110), Cu(100), Cu(111), Ag(100) and Ag(111) surfaces. We also show that using the local part of the full, screened, non-local pseudopotential can produce incorrect results for the binding energy of the image states. © 1997 Elsevier Science B.V.

Keywords: Alkali metals; Copper; Density functional calculations; Low index single crystal surfaces; Silver; Surface electronic phenomena

A metal surface generates electron states which do not exist in a bulk metal. Some of them are intrinsic surface states arising from the crystal potential termination and are localised mainly at the surface atomic layer [1,2]. States of another kind are linked to the long-range image potential $V(z) = -1/4(z - z_{\mathrm{im}})$ and are localised well outside the metal (at 2–50 Å from the image plane position z_{im}) [3–7]. In a hydrogenic model [3–7], these states form a Rydberg-like series

$$E_n = -0.85\ \mathrm{eV}/(n+2)^2. \quad (1)$$

The lifetime τ_i of the states scales asymptotically with the quantum number n [6]

$$\tau_i \propto n^3. \quad (2)$$

The parameter a depends on the surface of interest. In particular, it depends on the width of the energy gap and its position relative to the vacuum level.

The binding energies of image states have been measured by inverse photoemission [8–10], two-photon photoemission [11,12] and time-resolved photoemission [13] techniques. Measurements of the lifetime (intrinsic linewidth) have shown that the first and second image-state lifetime values deviate from Eq. (2) for real metal surfaces [11,13]. First-principles calculations of binding

* Corresonding author. Fax: +34 43 212236; e-mail: waptctce@sq.ehu.es

PII S0039-6028(97)00653-5

energies and lifetimes of the image states are very useful because they describe accurately the charge density and the potential in the bulk metal and at the surface. These calculations of image-state binding energies have been performed for the Cu(100) [14], Ni(100) [15], Fe(110) [16], Ag(100) [17], Al(100) [15,18,19] and Al(111) [19] surfaces. Similar calculations of the image-state lifetimes are restricted by the complexity of first-principles description of the screened Coulomb interaction [20–23]. On the other hand, the calculations [20,21] of lifetimes of the image states performed within the GW approximation [24] for the electron self-energy indicate that the overlapping of the image states with the bulk states is a crucial factor in the evaluation of the lifetime. Therefore, for practical calculations of the lifetime, a model including an accurate description of the binding energy and of the spatial behaviour of image states is needed.

In this Letter we present a first-principles calculation of the electronic structure of the Li(110) surface, including image potential states. We also present a one-dimensional model of the metal–vacuum system which reproduces accurately the width and the position of the energy gap at the $\bar{\Gamma}$ point and the energies E_0 and E_1 of the surface state and the first image state, respectively. We test the model for the Li(110) surface and later apply it to the calculation of binding energies and wave functions of image states on the Cu(100), Cu(111), Ag(100) and Ag(111) surfaces. The Li(110) surface has been chosen as a test system because on this surface at $\bar{\Gamma}$ a wide energy gap exists between the Fermi level and the vacuum level. Such a position of the energy gap is typical for many noble and transition-metal surfaces [25]. Just above the Fermi level, the electronic structure of the Li(110) surfaces is very similar to that of Cu(100) and Ag(100). At the same time, just below the vacuum level, the electronic structure of Li(110) is similar to that of Cu(111) and Ag(111). In particular, the first image state is located near the upper edge of the energy gap.

To calculate the electronic structure of the Li(110) surface, we use the self-consistent pseudopotential method and a supercell technique. In this technique, a unit cell consisting of a thin film of a metal and vacuum region is repeated in space to form the three-dimensional periodicity of the system. The norm-conserving non-local ion pseudopotential of lithium is generated according to Ref. [26]. We use a local density approximation (LDA) [27,28] for the exchange correlation potential. The calculations are carried out for nine-, 15-, 21- and 27-layer films. The final results are given for a 27-layer film. The self-consistent procedure is performed using the LDA. As the LDA does not produce the correct asymptotic potential behaviour in the vacuum, the final iteration is carried out using a modified potential which for $z<z_{\mathrm{im}}$ is the self-consistent LDA potential and for $z>z_{\mathrm{im}}$ is

$$V(z)=\frac{\exp[=-\lambda(z-z_{\mathrm{im}})]-1}{4(z-z_{\mathrm{im}})}. \tag{3}$$

The image plane position z_{im} is obtained as the centre of gravity of the charge density induced by a weak, static electric field. To generate an external electric field, a small portion of electron density is taken from the film and is located at the centre of each vacuum region as a thin sheet of negative charge with surface charge density σ. So, the whole supercell is neutral. A similar model was used in Ref. [29]. Together with the film, this thin sheet creates in the vacuum the electric field

$$\epsilon=4\pi\sigma. \tag{4}$$

To obtain the induced charge density profile, we use the fields $\epsilon=0.005$, 0.010 and 0.015 a.u. (1 a.u. $=5.14\times10^{7}$ eV cm^{-1}). The image plane position is determined as $z_{\mathrm{im}}=\lim z_{\mathrm{im}}(\epsilon)$ for $\epsilon\to0$, being 3.63 a.u. relative to the surface atomic layer. This value is in reasonable agreement with the value of $z_{\mathrm{im}}=3.74$ a.u. found in a jellium model [30] for the density parameter r_s corresponding to bulk lithium. Eguiluz et al. [18] used an approach based on an integral equation relating the exchange-correlation potential to the electron self-energy of many-body perturbation theory. This approach gives a smaller value of z_{im} than the uniform electric field method. For the Li(110) surface, this difference does not significantly influence the binding energy of the first image state (this influence is practically negligible for the

Table 1
The Li(110) surface

	Self-consistent calculation	Model potential	Screened local pseudo-potential part	Model potential (for modified energy gap)
E_0	+0.18	+0.18	–	–
E_1	−0.73	−0.73	−0.53	−0.51
E_2	−0.22	−0.22	−0.18	−0.17
E_3	–	−0.100±0.002	–	−0.082±0.002
E_4	–	−0.056±0.002	–	−0.048±0.002
Eedge$^{\text{lower}}$	−3.10	−3.1	−0.99	−0.99
Eedge$^{\text{lower}}$	−0.11	−0.11	+0.98	−0.98
z_{im} (a.u.)	3.63	3.23	3.63	3.24
τ_1	27.4	25.2	–	25.6
τ_2	–	46.5	–	102.3

Note: image potential states energies $E_1, \ldots, E_4$ (eV) and gap edges $E_{\text{edge}}^{\text{lower}}$, $E_{\text{edge}}^{\text{upper}}$ (eV) are expressed with respect to the vacuum level. The surface state energy E_0 (eV) is given relative to the Fermi level. The image plane positon z_{im} is expressed relative to the surface atomic layer. τ_i is the image potential state lifetime (fs).

second and higher terms of Rydberg series). A change in z_{im} of 0.5 a.u. brings a change of about 0.04 eV in E_1. A similar slight dependence of E_1 value on the image plane position was found by Nekovee and Inglesfield for Ni(100) [15].

The calculated electronic structure of the Li(110) surface along the symmetry directions of the surface Brillouin zone is shown in Fig. 1. As can be seen from Fig. 1, there are no occupied surface states on this surface. Above the Fermi level, wide energy gaps exist at the $\bar{\Gamma}$ point and along the $\overline{\text{PH}}$ symmetry line. At $\bar{\Gamma}$, an unoccupied resonance surface state is found just below the energy gap. The first and second image states are located inside the energy gap in the vicinity of the upper gap edge. Some characteristics of the Li(110) electronic structure are given in Table 1.

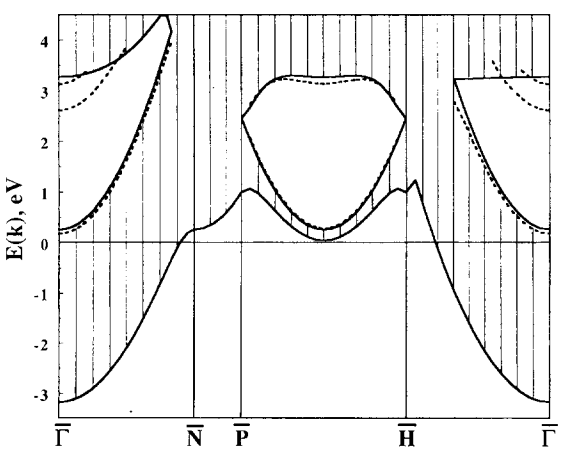

Fig. 1. Calculated surface electronic structure of Li(110): the projected bandstructure of bulk Li and the surface and image states (dashed line), $E_f=0$.

For a descriptipon of the surface electronic structure, we present a one-dimensional periodic-film model with large vacuum intervals the between films. In this model the full screened potential is given by

$$V_1(z)=A_{10}+A_1\cos\left(\frac{2\pi}{a_s}z\right), \quad z<D, \tag{5a}$$

$$V_2(z)=A_{20}+A_2\cos[\beta(z-D)], \quad D<z<z_1, \tag{5b}$$

$$V_3(z)=A_3\exp[-\alpha(z-z_1)], \quad z_1<z<z_{\text{im}}, \tag{5c}$$

$$V_4(z)=\frac{\exp[-\lambda(z-z_{\text{im}})]-1}{4(z-z_{\text{im}})}, \quad z_{\text{im}}<z. \tag{5d}$$

Here, D is the halfwidth of the film, and a_s is the interlayer spacing. The potential is continuous everywhere in space, together with its first derivative. It has ten parameters A_{10}, A_1, A_{20}, τ, A_3, α, Z_1, λ and z_{im}, and only four of them are independent. We chose A_{10}, A_1, A_2 and β as adjustable parameters. The first two parameters A_{10} and A_1 are determined from the requirement of describ-

ing the width and position of the energy gap at $\bar{\Gamma}$. The parameters A_2 and β must reproduce experimental or first-principles calculation values of E_0 and E_1 of the s–p-like surface state at $\bar{\Gamma}$ and the first image state, respectively. We use also the experimental or first-principles calculation work-function value to fix the Fermi level position relative to the vacuum level. For all the surfaces of interest, we use 400 layer films with 100 interlayer-spacing vacuum intervals between them. Such a geometry allows us to resolve resonance surface states on the Li(110), Cu(100), Ag(100) surfaces and resonance image states ($n=2$–4) on the Cu(111), Ag(111) surfaces with an accuracy better than 0.01 eV. In our model, the image plane position is not an adjustable parameter: it depends on the values of A_{10}, A_1, A_2 and β.

In Fig. 2a we show the one-dimensional potential (solid line) constructed for Li(110). Here we also present the local part of the full, screened, non-local pseudopotential averaged in the xy plane (dotted line). The origin of the discrepancy between these two curves is the use of the averaged local contribution, which presents only a part of the full, non-local pseudopotential. The averaged local contribution gives a different value of the energy gap and its position at the $\bar{\Gamma}$ point and different values of the binding energy of the image states (see Table 1). The model potential generated for the modified energy gap (for which we have changed only the parameters A_{10} and A_1) is very similar to the average local part of the pseudopotential. Both of them give practically the same energy values of the image states. This result confirms the important meaning of the energy gap for the description of image states found previously [3–9,31], and emphasises that using only the averaged local part of the screened non-local pseudopotential for a calculation of the binding energies of the image potential states can give incorrect results.

The squared wave function of the first image state calculated with the model potential for a 21-layer Li(110) film is shown in Fig. 2b (solid line). For comparison, we give here the squared wave function of the first image state obtained in the full pseudopotential calculation. As follows

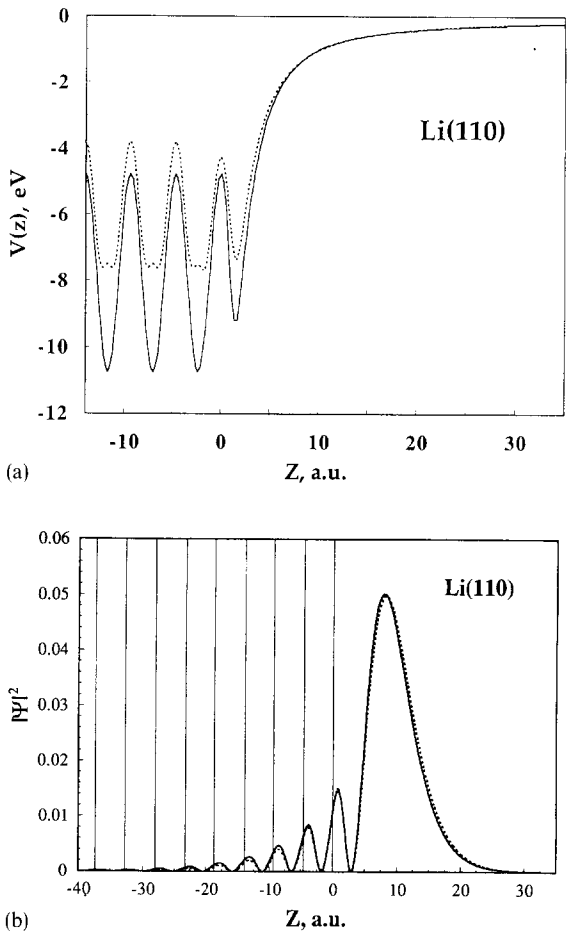

Fig. 2. (a) Model potential (solid line) and local pseudopotential part averaged in the xy plane (dotted line) of Li(110). (b) The first image-state wave-function square obtained from the model potential (solid line) and from the full pseudopotential (dotted line) calculation for a 21-layer Li(110) film.

from Fig. 2b, the discrepancy between the two curves is very small, especially in the vicinity of the surface atomic layer. A similar picture is observed for the surface resonance state and for the second image state. The results show that the proposed model potential describes binding energies and wave functions of the image states with high accuracy.

Applicaton of the model to the Cu(100), Cu(111), Ag(100) and Ag(111) surfaces gives the results presented in Tables 2 and 3. Comparison of the calculated wave functions of the image

Table 2
The Cu(100) and Cu(111) surfaces (designations and units correspond to those in Table 1)

	Cu(100)		Cu(111)	
	Experiment	Model potential	Experiment	Model potential
E_0	$+0.80^a$, $+1.15^b$, $+1.4^c$	+1.15	-0.39^g	−0.39
E_1	-0.578 ± 0.02^d	−0.57	-0.82 ± 0.05^h	−0.82
E_2	-0.18 ± 0.02^d	−0.18	-0.25 ± 0.07^h	−0.22
E_3	–	−0.083	–	-0.096 ± 0.004
E_4	–	−0.051	–	-0.054 ± 0.003
z_{im} (a.u.)	2.18^e	2.27	2.27^e	2.20
τ_1	23.5 ± 5^f	25.5	7.8 ± 1^f, 18 ± 5^h	5.6
τ_2	–	132	–	–

[a]Ref. [14], [b]Ref. [39], [c]Ref. [10], [d]Ref. [12], [e]Ref. [40], [f]Ref. [11], [g]Ref. [41], [h]Ref. [13].

Table 3
The Ag(100) and Ag(111) surfaces (designations and units correspond to those in Table 1)

	Ag(100)		Ag(111)	
	Experiment	Model potential	Experiment	Model potential
E_0	1.30 ± 0.1^a	−1.27	-0.07^f	−0.07
E_1	-0.53 ± 0.02^b	−0.53	-0.77 ± 0.03^b	−0.77
E_2	-0.16 ± 0.02^b	−0.17	-0.23 ± 0.03^b	-0.22 ± 0.01
E_3	-0.075^c	−0.081	0.10 ± 0.03^b-	-0.095 ± 0.005
E_4	–	−0.048	–	-0.053 ± 0.003
z_{im} (a.u.)	1.75^d	2.06	2.07^d	2.35
τ_1	31 ± 6^c, 25 ± 10^e	26.5	15 ± 3^c	6
τ_2	$178\pm20^{c,e}$	132	–	–

[a]Ref. [10], [b]Ref. [12], [c]Ref. [11], [d]Ref. [40], [e]Ref. [42], [f]Ref. [43].

states with those obtained from the first-principles calculations for Cu(100) [14] and Ag(100) [17] shows good agreement between the model potential and the first-principles results. Following Ref. [11], we can estimate the lifetime of the image states using a heuristic approximation. In this, the linewidth value of an image state is approximately determined as $\Gamma(E_i)=p_i\Gamma_b(E_i)$. Here, p_i is a portion of the ith image state wave function located in the bulk (i.e. the penetration value), and $\Gamma_b(E_i)$ is the linewdith of a bulk state corresponding to the energy $E-E_i$. Many experimental observations give a first-approximation linear dependence of the linewidth of bulk sp and d states on an energy relative to the Fermi level E_f [32–36]

$$\Gamma_b(E_i)=b(E_i-E_f). \quad (6)$$

This linear dependence is implemented for energies 5–50 eV above E_f. At the same time, conventional Landau Fermi-liquid theory gives quadratic dependence of the linewidth on an energy within 0–2 eV [37]. The image states on Cu and Ag surfaces have energies of 4–4.5 eV relative to E_f. So, for an estimation of the lifetime values of these states, we use the linear dependence (Eq. (6)). The image state energies of Li(110) have energies of 2.5–3 eV. In this case, we use the quadratic dependence of the linewidth of bulk states on the excitation energy. The coefficient b determined experimentally for Cu and Ag is equal to 0.13 [36]. For Li, the coefficient obtained from experimental mean free path data [38] is 0.025. The evaluated lifetime values $\tau_i=h/\Gamma(E_i)$ for some image states are pre-

sented in Tables 1–3. The results obtained are in good agreement with experimental data for the first image state on Cu(100) and Ag(100). For Cu(111) and Ag(111), we obtain only semi-quantitative agreement. Better agreement is observed with experimental data obtained from linewidth measurements than from direct measurements of the lifetime. The deviation of the calculated lifetime values from the experimental values for (111) surfaces arises from the specific character of the projection of the bulk bandstructure of Cu and Ag onto the (111) surface [25,44]. On this surface there are no direct transitions from the first image state (initial state) into the final unoccupied states. This means that the self-energy produces a smaller contribution to the linewidth of the image states and larger value of the lifetime in comparison with the case of the evaluation based on the penetration value only. At the same time, the projection of bulk bandstructure onto the (100) surface [14,25,44] provides direct transitions. In this case, the self-energy can give results close to that obtained according to the penetration value only. We believe that more accurate agreement with experimental data can be obtained by direct calculation of the self-energy with use of proposed potential. This work is in progress.

Acknowledgements

The authors are indebted to P. Apell and A. Arnau for reading of the manuscript and valuable comments. One of the authors (E.V.C.) is grateful to E. Zaremba, I. Nagy, A. Rivacoba, P. Apell, V. Ponce, A. Arnau, E.W. Plummer, E. Ortega, M. Wolf, M. Aeschlimann, M. Steslicka and L. Jurczyszyn for useful discussions. E.V.C. and V.M.S. thank the Departmento de Educacion del Gobierno Vasco and the Spanish Direccion General de Investigacion Cientifica y Technica (DGICYT) for financial support.

References

[1] I.E. Tamm, Z. Phys. 76 (1932) 849.
[2] W. Shockley, Phys. Rev. 56 (1939) 317.
[3] W.T. Sommer, Thesis, Stanford University, 1964.
[4] M. Cole, M.H. Cohen, Phys. Rev. Lett. 23 (1969) 1238.
[5] V.B. Shikin, Sov. Phys. JETP 31 (1970) 936.
[6] P.M. Echenique, J.B. Pendry, J. Phys. C 11 (1978) 2065.
[7] P.M. Echenique, J.B. Pendry, Prog. Surf. Sci. 32 (1990) 111.
[8] F.J. Himpsel, Comments Cond. Matter Phys. 12 (1986) 199.
[9] N.V. Smith, Rep. Prog. Phys. 51 (1988) 1227.
[10] F.J. Himpsel, J.E. Ortega, Phys. Rev. B 46 (1992) 9719.
[11] T. Fauster, W. Steinmann, in: P. Halevi (Ed.), Electromagnetic Waves: Recent Development in Research, vol. 2, Elsevier, Amsterdam, 1995, p. 350.
[12] K. Giesen, F. Hage, F.J. Himpsel, H.J. Riess, W. Steinmann, Phys. Rev. B 35 (1987) 971.
[13] M. Wolf, E. Knoesel, T. Hertel, Phys. Rev. B 54 (1996) R5295.
[14] S.L. Hulbert, P.D. Johnson, M. Weinert, R.F. Garrett, Phys. Rev. B 33 (1986) 760.
[15] M. Nekovee, J.E. Inglesfield, Europhys. Lett. 19 (1992) 535.
[16] M. Nekovee, S. Crampin, J.E. Inglesfield, Phys. Rev. Lett. 70 (1993) 3099.
[17] Z. Li, S. Gao, Phys. Rev. B 50 (1994) 15349.
[18] A.G. Eguiluz, M. Heinrichsmeier, A. Fleszar, W. Hanke, Phys. Rev. Lett. 68 (1992) 1359.
[19] V.M. Silkin, E.V. Chulkov, Fiz. Tverd. Tela 36 (1994) 736.
[20] P.M. Echenique, F. Flores, F. Sols, Phys. Rev. Lett. 55 (1985) 2348.
[21] P.L. de Andres, P.M. Echenique, F. Flores, Phys. Rev. B 35 (1987) 4529.
[22] J.J. Deisz, A. Eguiluz, W. Hanke, Phys. Rev. Lett. 71 (1993) 2793.
[23] J.J. Deisz, A. Fleszar, M. Heinrichsmeier, A.G. Eguiluz, unpublished.
[24] L. Hedin, S. Lundqvist, Solid State Phys. 23 (1969) 1.
[25] D.A. Papaconstantopouloss, The Band Structure of Elemental Solids, Plenum, New York, 1986.
[26] G.B. Bachelet, D.R. Hamann, M. Schluter, Phys. Rev. B 26 (1982) 4199.
[27] W. Kohn, L.J. Sham, Phys. Rev. 140 (1965) A1133.
[28] L. Hedin, B.J. Lundqvist, J. Phys. C 4 (1971) 2064.
[29] S.C. Lam, R.J. Needs, Surf. Sci. 277 (1992) 173.
[30] N.D. Lang, W. Kohn, Phys. Rev. B 7 (1973) 3541.
[31] N.V. Smith, Phys. Rev. B 32 (1985) 3549.
[32] A. Santoni, F.J. Himpsel, Phys. Rev. B 43 (1991) 1305.
[33] H.J. Levinson, F. Greuter, E.W. Plummer, Phys. Rev. B 27 (1983) 727.
[34] W. Eberhardt, E.W. Plummer, Phys. Rev. B 21 (1980) 3245.
[35] A. Goldmann, W. Altmann, V. Dose, Solid State Commun. 79 (1991) 511.
[36] D. Li, P.A. Dowben, J.E. Ortega, F.J. Himpsel, Phys. Rev. B 47 (1993) 12895.
[37] D. Pines, P. Nozieres, The Theory of Quantum Liquids, Benjamin, New York, 1996.

[38] G.K. Wertheim, D.M. Riffe, N.V. Smith, P.H. Citrin, Phys. Rev. B 46 (1992) 1995.
[39] D.P. Woodruff, S.L. Hulbert, P.D. Johnson, N.V. Smith, Phys. Rev. B 31 (1985) 4046.
[40] N.V. Smith, C.T. Chen, M. Weinert, Phys. Rev. B 40 (1989) 7565.
[41] S.D. Kevan, Phys. Rev. Lett. 50 (1983) 526.
[42] R.W. Schoenlein, J.G. Fujimoto, G.L. Eesley, T.W. Caperhart, Phys. Rev. B 43 (1991) 4688.
[43] R. Paniago, R. Matzdrof, G. Meister, A. Goldmann, Surf. Sci. 336 (1995) 113.
[44] S. Schuppler, N. Fisher, Th. Fauster, W. Steinmann, Phys. Rev. B 46 (1992) 13539.